

# Geophysical Research Letters<sup>®</sup>

## RESEARCH LETTER

10.1029/2024GL114321

### Key Points:

- The spatial trends of negative vegetation anomalies and drought frequency were similar
- Normal droughts are more destructive to vegetation health than flash droughts
- Flash droughts can rapidly induce water stress and intensify the effects of high temperatures within a short timeframe

### Supporting Information:

Supporting Information may be found in the online version of this article.

### Correspondence to:

Y. Xu,  
[xuyy@nju.edu.cn](mailto:xuyy@nju.edu.cn)

### Citation:

Liao, J., Xu, Y., Pi, J., Li, Y., Ke, C., Zhan, W., & Chen, J. (2025). Widespread sensitivity of Vegetation to the transition from Normal droughts to Flash droughts. *Geophysical Research Letters*, 52, e2024GL114321. <https://doi.org/10.1029/2024GL114321>

Received 18 DEC 2024

Accepted 7 MAR 2025

### Author Contributions:

**Conceptualization:** Jiangling Liao, Yuyue Xu

**Data curation:** Jiangling Liao

**Funding acquisition:** Yuyue Xu

**Methodology:** Jiangling Liao, Yuyue Xu

**Supervision:** Yuyue Xu

**Validation:** Yuyue Xu

**Writing – original draft:** Jiangling Liao, Yuyue Xu, Junzheng Pi, Yuchen Li, Changqing Ke, Wenfeng Zhan, Jianli Chen

**Writing – review & editing:**

Jiangling Liao, Yuyue Xu, Junzheng Pi, Yuchen Li, Changqing Ke, Wenfeng Zhan, Jianli Chen

© 2025. The Author(s).

This is an open access article under the terms of the [Creative Commons Attribution-NonCommercial-NoDerivs License](#), which permits use and distribution in any medium, provided the original work is properly cited, the use is non-commercial and no modifications or adaptations are made.

## Widespread Sensitivity of Vegetation to the Transition From Normal Droughts to Flash Droughts

Jiangling Liao<sup>1,2</sup>, Yuyue Xu<sup>1,2,3</sup> , Junzheng Pi<sup>1,2</sup>, Yuchen Li<sup>1,2</sup>, Changqing Ke<sup>1,2</sup> , Wenfeng Zhan<sup>4</sup> , and Jianli Chen<sup>5</sup> 

<sup>1</sup>School of Geography and Ocean Science, Nanjing University, Nanjing, China, <sup>2</sup>Jiangsu Provincial Key Laboratory of Geographic Information Science and Technology, Nanjing University, Nanjing, China, <sup>3</sup>Frontiers Science Center for Critical Earth Material Cycling, Nanjing University, Nanjing, China, <sup>4</sup>International Institute of Earth System Science, Nanjing University, Nanjing, China, <sup>5</sup>Department of Land Surveying and Geo-Informatics and Research Institute for Land and Space, The Hong Kong Polytechnic University, Kowloon, China

**Abstract** Global climate change has intensified flash droughts, which differ from traditional droughts, and have significant ecological impacts. However, differences in ecosystem responses to normal and flash droughts in China remain unclear, particularly in terms of vegetation vulnerability and resilience. Using a three-dimensional clustering method, we identified disparities between these drought types from 1982 to 2022 and found that flash droughts developed 40% faster than normal droughts, but normal droughts caused more severe vegetation damage. With the transition to flash droughts, vegetation sensitivity to droughts has increased. Using Shapley's additive interpretation method, we assessed the role of each environmental factor in vegetation recovery. The results show that in normal droughts, drought characteristics and vegetation sensitivity drive the resilience of vegetation, whereas in flash droughts, temperature and vapor pressure deficit become more significant. These insights provide a deeper understanding of vegetation resilience and drought tolerance under changing climatic conditions.

**Plain Language Summary** Global warming has intensified the transition from normal droughts to flash droughts, which are characterized by increased frequency and faster development. However, the impact of this transition on vegetation vulnerability and resilience remains poorly understood. In this study, we analyzed over 40 years of drought trends in China and found a significant increase in flash drought frequency, particularly in humid regions. Vegetation sensitivity showed similar spatial patterns to drought changes. Using an interpretable machine learning approach, we assessed the roles of drought characteristics, hydroclimatic factors, vegetation sensitivity, and other environmental conditions in vegetation recovery. Our results indicate that the drivers of vegetation restoration differ between normal and flash droughts, with drought duration having a greater impact than the rate of development. For flash droughts, temperature and vapor pressure deficit are key factors influencing recovery. These findings enhance our understanding of vegetation responses to climate change.

## 1. Introduction

Drought disrupts terrestrial ecological balance, leading to reduced vegetation productivity and increased tree mortality. As a key component of terrestrial ecosystems, vegetation is a crucial source of organic matter that plays a vital role in maintaining biospheric functioning. Anomalies in temperature, precipitation (PRE), soil moisture (SM), and vapor pressure deficits during drought can cause vegetation to experience water stress (T. Jiang et al., 2023), which usually results in stomatal closure (Sato et al., 2024). This closure slows the rate of photosynthesis, consequently reducing gross primary productivity (GPP) (Deng et al., 2021). Therefore, timely and accurate monitoring of widespread drought stress is essential to ensure food security and understand the responses of vegetation to climate change.

With global warming, the geographic extent of droughts has expanded, while occurring more frequently and shifting to wet areas (Ma & Yuan, 2024; Zheng et al., 2024). Droughts that occur frequently on subseasonal timescales and rapidly exert water stress on vegetation within a few weeks are termed “flash droughts” (Otkin et al., 2018; Yuan et al., 2023; Zhang & Yuan, 2020). Flash droughts primarily occur during the vegetation growing season in southern China and are spatially concentrated (Chen et al., 2019; Zhao et al., 2024). Compared to normal droughts, flash droughts not only shorten the warning time for mitigating the damage on vegetation

(Pendergrass et al., 2020), but are also often accompanied by other extreme weather events, including heat waves and strong winds (Zeng et al., 2023), which may have serious ecological and agricultural impacts (Zhao et al., 2024). For example, a flash drought outbreak in 2019 had a major impact on 2.35 million hectares of crops in southern China (Wang & Yuan, 2021), and reduced the GPP of vegetation in the Haihe River Basin by 40% (Yao, Liu, et al., 2022). Similarly, a mega-summer flash drought in the Yangtze River Basin in China in 2022 led to a notable reduction in GPP (Xi et al., 2024).

The response of vegetation to drought is influenced by various factors, including anomalies in climatic conditions, drought-tolerant properties of vegetation, and drought characteristics (Li, Zhang, et al., 2023c; Lu, Sun, Cheng, et al., 2024; Sungmin & Park, 2024). Changes in factors such as increased temperature (Wang & Yuan, 2023), excess radiation (Ford & Labosier, 2017), decreased SM (Li et al., 2022; Yao et al., 2023), and vapor pressure deficit (VPD) (Xi et al., 2024) during drought can impair vegetation growth and health (Eamus et al., 2013). Some of these factors determine the status of vegetation recovery from drought. Drought tolerance and vegetation resilience are also influenced by ecosystem type and environmental conditions (Schwalm et al., 2017; Yao, Fu, et al., 2022; Zhang et al., 2024). For example, vegetation in arid and semi-arid regions exhibits greater drought tolerance and resilience owing to long-term adaptation to moisture-limiting conditions (Cao et al., 2022; Xu et al., 2018). Conversely, humid areas may face more pressing drought risks than water-scarce areas because of increasing drought frequency trends (Li, An, et al., 2024). Differences in the characteristics and accompanying hydrometeorological conditions between normal and flash droughts can result in differences in vegetation response (Corak et al., 2024). As flash droughts have emerged as a significant research hotspot, many studies have focused on comparing them with normal droughts, and examining their characteristics and climate change impacts (Guo et al., 2024; Ho et al., 2023). However, the distinct roles played by normal and flash droughts on vegetation remain unclear. Further investigations are needed to understand how these drought types differentially influence plant health and ecology, which are essential for effective management and resilience strategies.

In response to the above mentioned research gaps, we characterized normal and flash droughts using a three-dimensional clustering method (Xu et al., 2015) and explored the differential effects on vegetation using the Standardized Soil Moisture Index (SSMI) and remotely sensed vegetation indices from 1982 to 2022 in China. To analyze the sensitivity of various vegetation types to drought events, we quantified drought resistance (Relative Frequency (RF) and lag (Relative Lag Time (RLT) indices (Jin et al., 2023). Then, we revealed the main drivers of vegetation Recovery Duration (RD) from normal and flash droughts using Shapley's additive interpretation (SHAP) method in random forest modeling and explored the spatial distribution of the dominant drivers of recovery time by applying partial correlation analysis.

## 2. Materials and Methods

### 2.1. Materials

#### 2.1.1. Soil Moisture and Hydro-Meteorological Data

SM was calculated using root zone SM data averaged from three data sets, ERA5, GLDAS v2.0, v2.2/Catchment, and Global Land Evaporation Amsterdam Model (GLEAM) v3.8a, covering depths from 0 to 100 cm. To mitigate excessive fluctuations in surface SM data, we employed root zone SM data from depths of 0–100 cm (Ford & Labosier, 2017). Soil moisture data of ERA5 were obtained from the European Centre for Medium-Range Weather Forecasts (ECMWF) Integrated Forecasting System (IFS), which categorizes the soil into four layers: layer 1 (0–7 cm), layer 2 (7–28 cm), layer 3 (28–100 cm), and layer 4 (100–289 cm). We used the first three layers of SM data and interpolated them for the 0–100 cm data (Sungmin & Orth, 2021). The SM data of the Global Land Data Assimilation System (GLDAS) include four depth layers, with the 0–100 cm layer being the most effective for assessing SM in the root zone of vegetation. The GLEAM is another comprehensive global data set designed to estimate land evaporation and root-zone SM using satellite data.

The hydro-meteorological elements analyzed in this study, included PRE, potential evapotranspiration, solar radiation (RAD), maximum temperature ( $T_{\max}$ ), VPD, sensible heat flux (SHF), and latent heat flux (LHF). The PRE, RAD, and  $T_{\max}$  were obtained from the ERA5, and the SHF and LHF were obtained from the data of the GLDAS model.

### 2.1.2. Remote Sensing Vegetation Indices

We quantitatively analyzed vegetation growth during drought using three complementary vegetation growth indices: the Normalized Vegetation Index (NDVI), Leaf Area Index (LAI), and Solar-Induced Chlorophyll Fluorescence (SIF). The NDVI is widely recognized as a measure of vegetation greenness. We used biweekly NDVI data from the Peking University (PKU) Global Inventory Modeling and Mapping Studies (GIMMS) NDVI data set, which has a resolution of  $0.25^\circ$ , spanning 1982 to 2022 (Li et al., 2023a). The LAI effectively captures structural changes in vegetation under drought stress. The data for this analysis were downloaded from the GIMMS LAI4g data set (Cao et al., 2023), which provided biweekly global LAI data at a resolution of  $1/12^\circ$  from 1982 to 2020. Additionally, LAI data for 2021–2022, released by Pu et al. (2024), were used. The SIF provides another perspective for examining the effects of drought on vegetation photosynthesis. Solar-Induced Chlorophyll Fluorescence data were sourced from global “OCO-2” SIF data set (GOSIF) (Li & Xiao, 2019), which offers global chlorophyll fluorescence data at  $0.05^\circ$  over 8-day intervals from 2002 to 2022.

## 2.2. Methods

### 2.2.1. Three-Dimensional Drought Identification

We identified droughts using a three-dimensional clustering method and distinguished flash droughts from normal droughts in terms of rate of onset and duration (Ji & Yuan, 2024; Yuan et al., 2019). The method of recognizing normal and flash drought events based on 3D clustering is described in detail in Ho et al. (2023) and Li, Wang, et al. (2020) and is now summarized:

*Drought Patch Identification:* A drought patch was defined as a cluster of neighboring pixels with the SSMI less than a specified drought threshold ( $SSMI \leq -1$ ). The SSMI was calculated based on the methodology described by Hao et al. (2017) on a pentad timescale, where a pentad is 5 days. Additionally, the area of these neighboring clustered pixels must exceed a designated area threshold ( $\text{area} \geq 50,000 \text{ km}^2$ , Text S3) (Lloyd-Hughes, 2012; Su et al., 2018; Wang et al., 2011).

*Temporal Continuity of Drought Patches:* Two drought patches were considered to be temporally part of the same event if the area of overlap between a drought patch at the current time and a drought patch at a previous time step exceeded 50% of the area of the smaller drought patch.

*Drought Event Duration Limit:* The minimum drought duration was set as greater than or equal to five pentads, whereas the maximum duration was set as less than 165 pentads. Flash droughts were defined as those with durations ranging from 5 to 18 pentads.

*Drought Event Severity:* Drought patch loss (Severity<sub>*i*</sub>) was defined as the cumulative SSMI value of all pixels within a drought patch. The severity of a drought event was the sum of all drought patch losses during the event. The intensity of the drought event was determined by the largest drought patch loss within the event using the absolute maximum value of Severity<sub>*i*</sub>. The formulas are as follows:

$$\text{Severity}_i = \sum_{j=1}^N \text{SSMI}_{ij} \quad (1)$$

$$\text{Severity} = \sum_{i=1}^M \text{Severity}_i \quad (2)$$

$$\text{Intensity} = \max_{i=1}^M (|\text{Severity}_i|) \quad (3)$$

where Severity<sub>*i*</sub> represents the loss in the *i*-th drought patch. SSMI<sub>*ij*</sub> is the SSMI of the *j*-th pixel in the *i*-th drought patch. Where *N* is the total number of pixels in the *i*-th drought patch. *M* refers to the total number of drought patches involved in a drought event.

*Definition of Development and Recovery Phases:* The recovery moment (*p*) was defined as the time at which the drought event reached its peak intensity. Using recovery moment (*p*) as a dividing point, the drought was divided into 2 phases, with the first half being the development phase and the second half being the recovery phase.

*Limit of Development Speed of Flash Drought:* The average rate of instantaneous intensification (AIIR) during the development phase of a flash drought should be less than or equal to 45% of the cumulative distribution frequency

of each instantaneous intensification rate (IIR) during that stage. To establish this, the IIR in the drought development phase was first calculated, followed by computation of the AIIR for the development phase:

$$\text{IIR}_{(i,i+1)} = \text{Severity}_{i+1} - \text{Severity}_i \quad (4)$$

$$\text{AIIR} = \frac{\sum_{i=1}^{p-2} \text{IIR}}{p-2} \quad (5)$$

where  $p$  is the recovery moment and  $i$  and  $i+1$  are the time steps.

### 2.2.2. Vegetation Response to Drought

There are three features of vegetation response to drought, as illustrated in Figure S1 in Supporting Information S1: (a) *Frequency of Negative Vegetation Anomalies*: A negative vegetation anomaly during a drought event was defined as the remotely sensed vegetation index falling below  $-0.5$  standard deviations ( $z\text{-score} \leq -0.5$ ). The frequency of negative vegetation anomalies was calculated as the number of anomalies observed across all drought events. (b) *Lag Time of Vegetation Response to Drought (LT)*: This was defined as the duration from the onset of the drought event ( $\text{SSMI} \leq -1$ ) to the point when vegetation levels dropped below the specified negative anomaly threshold ( $z\text{-score} \leq -0.5$ ). (c) *Recovery Duration (RD)*: This duration lasted from the peak of vegetation loss until the vegetation returned to its normal levels. ( $z\text{-score} > -0.5$ ).

Vegetation exhibits a degree of resistance to water stress, resulting in a lag time when the onset of vegetation anomalies occurs after the onset of drought. We evaluated the sensitivity of vegetation to drought events by examining the drought resistance and lag times. Drought resistance was quantified as the ratio of the frequency of negative vegetation anomalies to the frequency of drought events. Additionally, we defined hysteresis as the ratio of the lag time of vegetation response to drought to the duration of the drought. These metrics were termed RF and RLT. A smaller RF indicates greater resistance of vegetation to drought, whereas a larger RLT signifies a longer delay in the vegetation response to drought.

### 2.2.3. Attributional Analysis

To analyze the drivers of recovery time for different vegetation types under normal and flash drought conditions, we applied a random forest model to assess the contributions of vegetation sensitivity, drought characteristics, and a range of climatic, biological, and soil factors to vegetation recovery. Separate random forest models were constructed for each of the following 10 groups: vegetation recovery patterns under two scenarios, normal drought and flash drought, across five vegetation types (evergreen forests, deciduous forests, shrublands, grasslands, and croplands, Figure S2 in Supporting Information S1). For vegetation sensitivity, we selected RF and RLT as the key metrics. In terms of drought characteristics, we focused on the severity and duration of drought events. We employed several indicators of climate, including PRE, temperature, VPD, and SHF. Additionally, for biological and soil factors, we analyzed aboveground forest biomass, and soil sand and soil clay contents.

Random forest regression and SHAP values were used to rank the importance of drivers influencing vegetation recovery. To efficiently search for optimal hyperparameters, we used a “random search” strategy with 1,000 iterations and assessed model performance with 60/40 splitting and 10-fold cross-validation. SHAP values were used to interpret the contribution of each feature to the prediction. We also employed partial dependent plots to visualize the response functions associated with vegetation recovery time, offering a clearer picture of how changes in predictor variables affect recovery. In addition, we used a partial correlation analysis to determine the spatial patterns of dominant factors by calculating partial correlation coefficients within spatially shifted windows of varying sizes to enhance the robustness of the results. This multifaceted approach provided a comprehensive framework for analyzing the intricate relationships among drivers of vegetation recovery.

### 3. Results

#### 3.1. Characteristics of Normal and Flash Droughts

During the growing seasons from 1982 to 2022, 491 drought events were identified in China, comprising 327 normal droughts and 164 flash droughts. The average duration of normal droughts was 19.93 pentads with a recovery time of 9.03 pentads. In contrast, flash droughts had an average duration of 9.04 pentads and an average recovery time of 3.53 pentads. Normal droughts typically exhibit greater intensity and severity, leading to larger affected areas and longer durations than flash droughts. However, the rate of development of flash droughts, indicated by an AIIR of 140.39, was approximately 40% faster than that of normal droughts, which had an AIIR of 98.72 (Table S1 in Supporting Information S1).

From 1982 to 2022, there was a decline in the frequency of normal droughts and an increase in the frequency of flash droughts (Figure S3 in Supporting Information S1). This finding aligns with those of previous studies (Lu, Sun, Cheng, et al., 2024; Yuan et al., 2023). The increasing frequency of droughts was pronounced in humid regions. In the lower reaches of the Yellow River, the North China Plain, and Southeast China, the increase in frequency of flash droughts was substantial (Figure S4 in Supporting Information S1). The spatial distributions of the duration and RD for normal and flash droughts varied significantly. Normal droughts exhibited longer durations and recovery times in the semi-arid and humid regions of China. The average duration ranged from 8 to 24 pentads, whereas the recovery time ranged from 6 to 15 pentads. The mean duration of the flash droughts was primarily between 5 and 8 pentads, with recovery taking 2 to 3 pentads (Figure S5 in Supporting Information S1).

#### 3.2. Characterization of Vegetation Response to Normal and Flash Droughts

To assess the response of vegetation to drought, we analyzed three key features: the frequency of negative vegetation anomalies, vegetation lag time, and recovery time. The trend in the frequency of negative vegetation anomalies during droughts was similar to that of drought frequency, with a significant increase in frequency in humid areas (Figures S6 and S7 in Supporting Information S1). The lag time of vegetation in response to normal drought was within 2 months, and the recovery time was within half a year. In contrast, the average lag time for vegetation in response to flash droughts was approximately 1 month, and the recovery time was shorter than the lag time, ranging from one-half to 1 month (Figure S8 in Supporting Information S1). Ecosystems can maintain a certain degree of stability during drought. We found that the RF during normal droughts was greater than that during flash droughts, whereas the RLT was smaller for normal droughts than for flash droughts (Figure 1). The combination of a smaller RF, longer RLT, and longer recovery time associated with normal droughts suggests that normal droughts are more destructive to vegetation health than flash droughts.

The observed decrease in RF and increase in RLT from semi-arid to humid regions indicate greater drought tolerance in humid environments (L. L. Jiang et al., 2024). In humid areas, vegetation exhibited the highest RLT in response to drought, particularly under flash drought conditions (Figure 1c). One reason for the lower RF in hyper-arid and arid regions is that extremely dry conditions hinder vegetation growth, making it challenging to accurately characterize ecological changes during droughts using vegetation proxy indices. Drought resistance and lag time varied among different vegetation types. Evergreen forests and shrublands demonstrated greater drought resistance, characterized by smaller RF and larger RLT. In contrast, croplands showed greater sensitivity to drought, exhibiting higher RF and lower RLT values. This indicates that the drought tolerance of croplands was significantly weaker than that of other vegetation types, particularly to flash droughts. The smaller RLT for croplands highlights the challenges of mitigating drought damage in agriculture (Figure 1f). Additionally, the characteristics of vegetation responses to drought based on LAI and SIF calculations were similar to those based on the NDVI. During normal droughts, NDVI and LAI slightly outperformed SIF, whereas SIF showed a larger RF during flash droughts, likely due to the rapid restriction of photosynthesis in vegetation (Figure S9 in Supporting Information S1).

#### 3.3. Attribution of Recovery Duration for Normal and Flash Droughts

The random forest regression model demonstrated strong performance in capturing vegetation recovery, explaining 72.22% of the out-of-bag variance in recovery time for normal droughts and 62.68% for flash droughts. During normal droughts, the RD varied widely among vegetation types, with deciduous forests and shrublands demonstrating the longest RD. Notably, deciduous forests required considerably longer recovery time than other

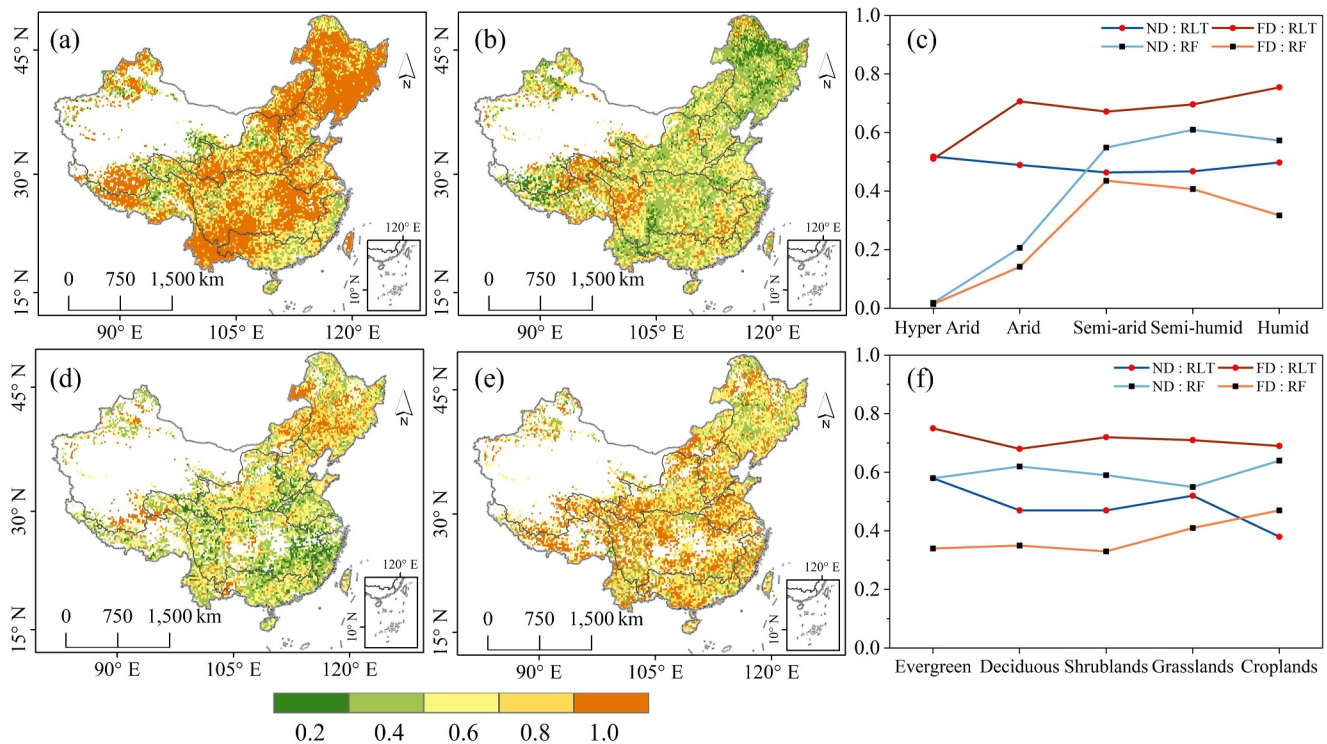


**Figure 1.** Drought resistance and hysteresis of vegetation in response to drought. (a) and (d) show the spatial distributions of Relative Frequency (RF) and Relative Lag Time (RLT) of vegetation to normal drought; (b) and (e) show the spatial distributions of RF and RLT of vegetation to flash drought; (c) show the RF and RLT in different climatic zones; and (f) show the RF and RLT of different vegetation types. Note: ND denotes normal drought, and FD denotes flash drought.

vegetation types. Interestingly, a prolonged lag time for vegetation corresponded to a shorter recovery time (Figure S10c in Supporting Information S1). Conversely, vegetation with high drought tolerance, as indicated by smaller RF values, took longer to recover when experiencing drought (Figure S10e in Supporting Information S1). The recovery time for vegetation from flash droughts typically ranged from 0.5 to 1 month. Vegetation that exhibited a longer lag time recovered faster (Figure S11a in Supporting Information S1). As the severity (Figure S11b in Supporting Information S1) and duration (Figure S11c in Supporting Information S1) of the flash drought increased, the recovery time for vegetation increased. Temperature significantly influenced vegetation recovery from flash drought, with a bimodal distribution, indicating that both low and high temperatures prolonged the recovery time (Figure S11d in Supporting Information S1). The relationship between recovery time and RF was not monotonic. Each vegetation type exhibited optimal recovery at an RF between 0.3 and 0.5 (Figure S11e in Supporting Information S1). Aboveground biomass exerted a considerable impact on croplands, and increased biomass was correlated with longer recovery time. Conversely, for other vegetation types, increased biomass was associated with shorter recovery time (Figure S11f in Supporting Information S1). This disparity may be attributed to the influence of anthropogenic factors on croplands.

During a normal drought, the recovery time was primarily determined by drought characteristics and the sensitivity of vegetation to drought. This underscores the significance of species composition and environmental background conditions in drought recovery (Sungmin & Park, 2024). Conversely, during flash droughts, the influence of drought characteristics on recovery time diminished, whereas the roles of PRE, temperature, and VPD became more significant (Figure 2). This demonstrates how flash droughts can cause rapid water stress and exacerbate high-temperature effects within a short period (Yin et al., 2023). Therefore, the threat posed to vegetation by flash droughts should not be underestimated.

### 3.4. Spatial Distribution of Dominant Factors of Vegetation Recovery

RLT, RF, temperature, VPD, and SM were significant factors influencing vegetation recovery. We conducted a partial correlation analysis to assess the effects of these factors on vegetation recovery across different regions.

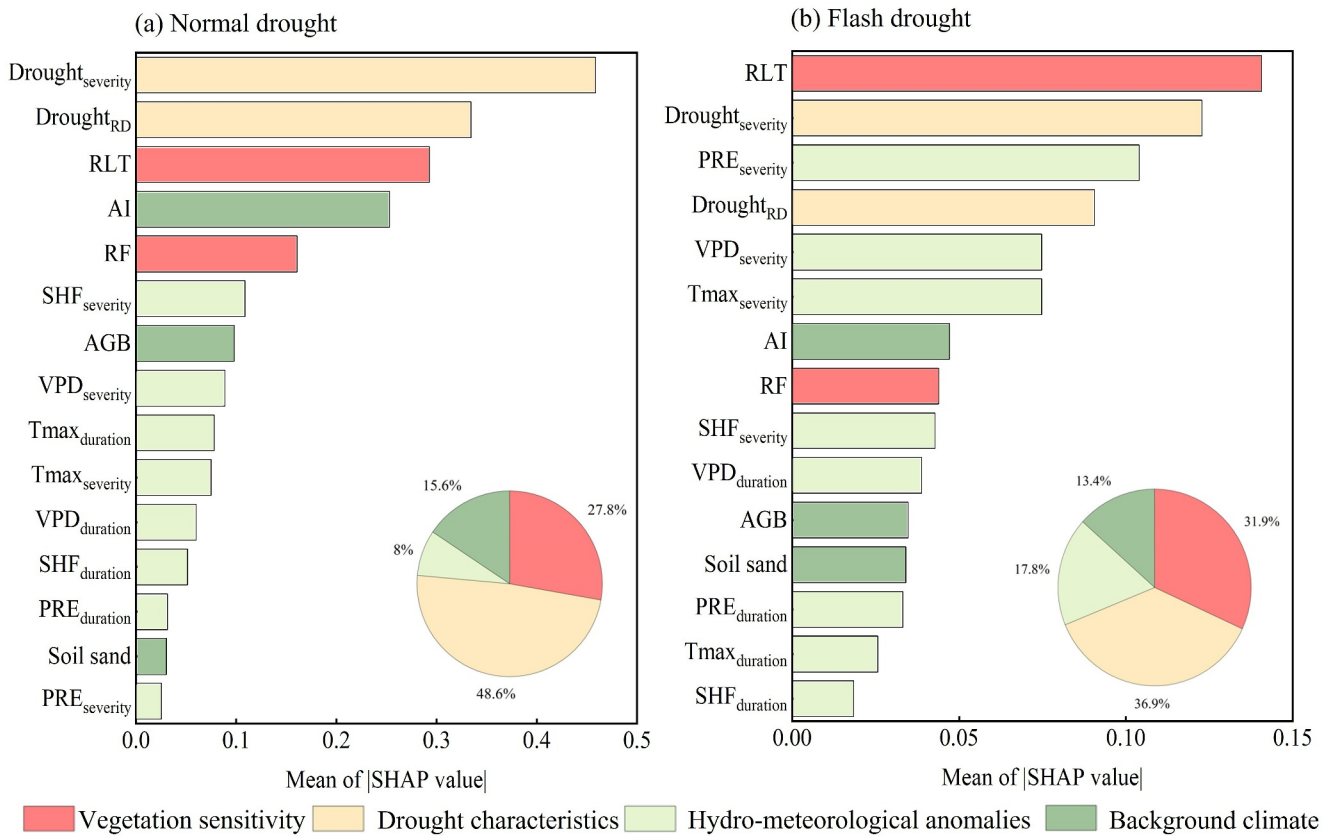


**Figure 2.** Ranking of key drivers of vegetation recovery calculated from the mean of absolute Shapley's additive interpretation values. (a) Shows the importance ranking of key variables for normal drought conditions, with the pie chart illustrating the normalized percentage contributions of the four variable categories; (b) shows the importance ranking of key variables for flash drought conditions, with the pie chart depicting the normalized percentage contributions of the four variable categories. The four variable categories include vegetation sensitivity, drought characteristics, hydro-meteorological anomalies, and background climate.

Our analysis revealed that RLT was the dominant driver of vegetation recovery during normal droughts, exerting an influence of 16.21%. This was followed by temperature, which had an influence of 5.47% (Figure 3c). A negative correlation between recovery time and RLT was observed in 70% of areas dominated by RLT. This trend was particularly pronounced in the middle and lower reaches of the Yangtze River and southwest China. In contrast, vegetation recovery time was primarily positively correlated with conditions of high temperature, high VPD, and low SM, accounting for 75%, 69%, and 82%, respectively (Figure S12 in Supporting Information S1). The effect of temperature was mainly observed in the middle and lower reaches of the Yangtze River and northern China. The impacts of VPD were concentrated in the upper reaches of the Yellow River and the middle and upper reaches of the Yangtze River, while the effects of SM were most significant in inland areas of China (Figure 3a, and Figure S12).

RLT also played a dominant role in flash droughts, primarily affecting areas in southwest China, the upper reaches of the Yangtze River, and the middle reaches of the Yellow River. The areas where temperature was positively correlated with recovery time were mainly located in the lower reaches of the Yangtze River and in parts of northern and northeastern China. Positive correlations between VPD anomalies and recovery times were concentrated in the middle and upper reaches of the Yangtze and Yellow Rivers. Additionally, areas showing positive correlations between SM loss and vegetation recovery time were primarily located in northwestern China. In contrast, RF had the smallest impact area, and its correlation with vegetation recovery time was not significantly biased (Figures 3b, 3d, Figure S13).

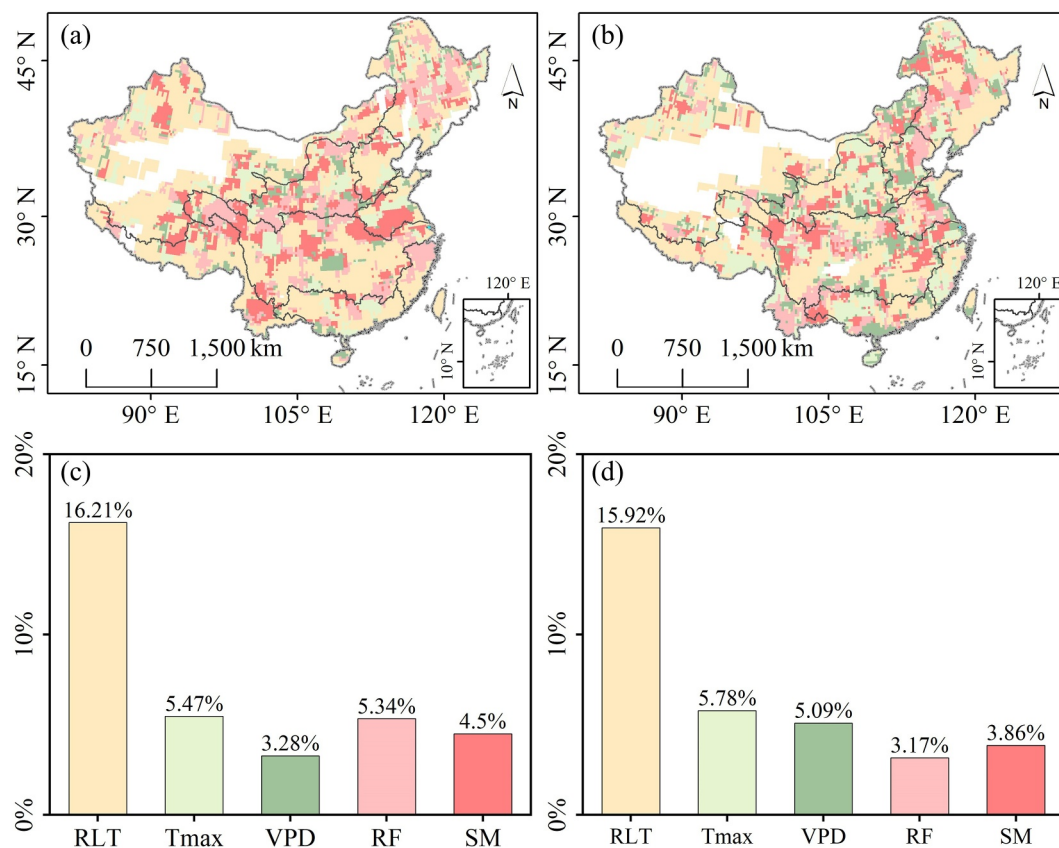


**Figure 3.** Spatial distribution of dominant factors in vegetation recovery time from drought. (a) Shows the spatial distribution of dominant factors during normal drought; (b) shows the spatial distribution of dominant factors during flash drought. (c) Presents the percentage of each dominant factor under normal drought, while (d) shows the percentage of each dominant factor under flash drought. Dominant factors include the RLT, temperature ( $T_{max}$ ), vapor pressure deficit, the RF, and soil moisture.

#### 4. Discussion

In this study, we successfully identified most historical drought events, including the drought events that occurred in 2010–2011 (Xu et al., 2015); and the mega-flash drought in southern China in 2022 (Liang et al., 2023). We concluded that the duration of a flash drought should range from 5 to 18 pentads and the average rate of the development stage should exceed 45% of the cumulative distribution frequency of each rate of change, which could be better applied to each region in China. For the area threshold of 3D drought identification, we tested four different thresholds, ranging from 25,000 to 150,000 km<sup>2</sup>, and found that the number of drought events was consistently in the hundreds (Table S2 in Supporting Information S1). While we identified droughts based on SM, other definitions of flash drought exist, such as the standardized evapotranspiration stress ratio (Christian et al., 2021). If accompanied by high temperatures and strong winds, some drought events may affect crop growth despite their short duration (1 or 2 pentads); however, these scenarios are beyond the scope of our discussion. The impact of increasing flash drought frequency on vegetation sensitivity remains debated, but it is clear that vegetation in humid regions faces greater drought risk (Li, Yang, et al., 2024; Tang et al., 2024). Our findings suggest that vegetation is more sensitive to normal droughts than flash droughts. This may be attributed to the lower sensitivity of vegetation to drought on shorter timescales, as the anomalies shown by the SSMI may not correspond to actual plant water deficits. Additionally, energy, rather than water, is the primary growth constraint for vegetation in the initial stages of drought in humid regions, where sufficient SM is still available but temperature and RAD can limit growth (Ho et al., 2023; Ma & Yuan, 2024). Grasslands and evergreen forests are tolerant to drought, whereas croplands are particularly sensitive, especially with a short lag time, consistent with the results of Deng et al. (2021).

We focused on the effects of vegetation sensitivity, drought characteristics, climatic factors, and soil texture on vegetative resilience. However, anthropogenic factors (Van Loon et al., 2016; Yin et al., 2023), such as irrigation, as well as other potentially influencing elements, including canopy structure, vegetation phenology, and nutrient availability, may also affect vegetation recovery processes. For instance, shallow-rooted plants are susceptible to climate change impacts and anthropogenic disturbances (Tariq et al., 2024), whereas the response time of vegetation to drought is prolonged as plant rooting depth increases (Lu, Sun, Yang, et al., 2024). The loss of leaf area and stored non-structural carbohydrates during drought can impair growth in subsequent years (Mueller & Bahn, 2022). Droughts associated with extremely high temperatures negatively affect carbon uptake (Gampe et al., 2021), slowing the absorption of carbon dioxide and nitrogen fertilizers by vegetation in terrestrial ecosystems. Additionally, the decline in vegetation cover is not only caused by the continued lack of water available to ecosystems; wildfires (Xu et al., 2024), hail, and floods can also significantly impact vegetation greenness and cover.

## 5. Conclusions

By analyzing drought events during the growing season in China from 1982 to 2022, we compared the responses of vegetation under normal and flash drought conditions. The results showed that the sensitivity of vegetation to drought has been widespread in China for more than 40 years. In the trend from normal drought to flash drought, the duration and severity of drought affected vegetation more than the rate of drought development. However, the extreme weather phenomena accompanying flash droughts can also damage vegetation within a few weeks. Normal droughts caused more long-term damage, leading to longer recovery times, whereas flash droughts had lower frequencies and longer relative lag times. The response of vegetation to drought is similar to the spatial pattern of drought trends, with good drought resistance of vegetation in humid areas. Anomalies in vegetation, especially in croplands, caused by the frequency of flash droughts in humid areas, should not be ignored. In addition, variations in drought tolerance were observed among different vegetation types, with evergreen forests and grasslands showing strong drought tolerance and croplands demonstrating greater sensitivity. This study provides valuable insights for understanding the effects of the rate of drought development on ecosystems and serves as a basis for implementing appropriate drought-resistant measures tailored to different vegetation types.

## Data Availability Statement

The ERA5 hourly reanalysis data sets from the ECMWF Integrated Forecasting System (IFS) can be downloaded from Sabater (2019). GLDAS Catchment Land Surface Model L4 daily data sets are available from Li, Beaudoin, et al. (2020). The GLEAM v3.8a data set can be accessed via Martens et al. (2017). The PKU GIMMS NDVI data set can be downloaded from Li et al. (2023b). The LAI data can be obtained from Pu et al. (2023) and Yan et al. (2023). The GOSIF data can be downloaded from Li and Xiao (2019). The MODIS land cover data set can be downloaded from Friedl and Sulla-Menashe (2015).

## References

- Cao, S., Li, M., Zhu, Z., Wang, Z., Zha, J., Zhao, W., et al. (2023). Spatiotemporally consistent global dataset of the GIMMS leaf area index (GIMMS LAI4g) from 1982 to 2020 [Article; Data Paper]. *Earth System Science Data*, 15(11), 4877–4899. <https://doi.org/10.5194/essd-15-4877-2023>
- Cao, S., Zhang, L., He, Y., Zhang, Y., Chen, Y., Yao, S., et al. (2022). Effects and contributions of meteorological drought on agricultural drought under different climatic zones and vegetation types in Northwest China. [Article]. *Science of the Total Environment*, 821, 153270. <https://doi.org/10.1016/j.scitotenv.2022.153270>
- Chen, L. G., Gottschalk, J., Hartman, A., Miskus, D., Tinker, R., & Artusa, A. (2019). Flash drought characteristics based on US drought monitor. *Atmosphere*, 10(9), 498. <https://doi.org/10.3390/atmos10090498>
- Christian, J. I., Basara, J. B., Hunt, E. D., Otkin, J. A., Furtado, J. C., Mishra, V., et al. (2021). Global distribution, trends, and drivers of flash drought occurrence. *Nature Communications*, 12(1), 6330. <https://doi.org/10.1038/s41467-021-26692-z>
- Corak, N. K., Otkin, J. A., Ford, T. W., & Lowman, L. E. L. (2024). Unraveling phenological and stomatal responses to flash drought and implications for water and carbon budgets. *Hydrology and Earth System Sciences*, 28(8), 1827–1851. <https://doi.org/10.5194/hess-28-1827-2024>
- Deng, Y., Wang, X. H., Wang, K., Ciais, P., Tang, S. C., Jin, L., et al. (2021). Responses of vegetation greenness and carbon cycle to extreme droughts in China. *Agricultural and Forest Meteorology*, 298, 108307. <https://doi.org/10.1016/j.agrformet.2020.108307>
- Eamus, D., Boulain, N., Cleverly, J., & Breshears, D. D. (2013). Global change-type drought-induced tree mortality: Vapor pressure deficit is more important than temperature per se in causing decline in tree health. *Ecology and Evolution*, 3(8), 2711–2729. <https://doi.org/10.1002/ece3.664>
- Ford, T. W., & Labosier, C. F. (2017). Meteorological conditions associated with the onset of flash drought in the Eastern United States. *Agricultural and Forest Meteorology*, 247, 414–423. <https://doi.org/10.1016/j.agrformet.2017.08.031>

## Acknowledgments

This study was supported by the National Key Research and Development Program of China (no. 2022YFF0711603), the AI & AI for Science Project of Nanjing University (no. 0209–14380140), the Frontiers Science Center for Critical Earth Material Cycling Fund (JBGS2102), National Natural Science Foundation of China (no. 41671423 and 42394132), the Hong Kong RGC Collaborative Research Fund (C5013-23G), and the Ministry Science and Technology Development of China-Data Sharing Infrastructure of Earth System Science (no. 2005DKA32300).

- Friedl, M., & Sulla-Menashe, D. (2015). MCD12C1 MODIS/Terra+Aqua land cover type yearly L3 global 0.05Deg CMG. NASA LP DAAC [Dataset]. *Boston University and MODAPS SIPS - NASA*. <https://doi.org/10.5067/MODIS/MCD12C1.006>
- Gampe, D., Zscheischler, J., Reichstein, M., O'Sullivan, M., Smith, W. K., Sitch, S., & Buermann, W. (2021). Increasing impact of warm droughts on northern ecosystem productivity over recent decades. *Nature Climate Change*, *11*(9), 772–779. <https://doi.org/10.1038/s41558-021-01112-8>
- Guo, H., Tian, Y. F., Li, J. L., Meng, X. C., Lv, X. Y., Wang, W., et al. (2024). Unveiling the spatiotemporal impacts of the 2021 central asian drought on vegetation: A comprehensive quantitative analysis. *Ecological Indicators*, *165*, 112238. <https://doi.org/10.1016/j.ecolind.2024.112238>
- Hao, Z. C., Hao, F. H., Singh, V. P., Ouyang, W., & Cheng, H. G. (2017). An integrated package for drought monitoring, prediction and analysis to aid drought modeling and assessment. *Environmental Modelling and Software*, *91*, 199–209. <https://doi.org/10.1016/j.envsoft.2017.02.008>
- Ho, S., Buras, A., & Tuo, Y. (2023). Comparing agriculture-related characteristics of flash and normal drought reveals heterogeneous crop response. *Water Resources Research*, *59*(11), e2023WR034994. <https://doi.org/10.1029/2023wr034994>
- Ji, P., & Yuan, X. (2024). Disparities and similarities in the spatiotemporal dynamics of flash and slow droughts in China. *Environmental Research Letters*, *19*(8), 084015. <https://doi.org/10.1088/1748-9326/ad5d7e>
- Jiang, L. L., Liu, B., Guo, H., Yuan, Y., Liu, W. L., & Jiapaer, G. (2024). Assessing vegetation resilience and vulnerability to drought events in Central Asia. *Journal of Hydrology*, *634*, 131012. <https://doi.org/10.1016/j.jhydrol.2024.131012>
- Jiang, T., Su, X., Zhang, G., Zhang, T., & Wu, H. (2023). Estimating propagation probability from meteorological to ecological droughts using a hybrid machine learning copula method. [Article]. *Hydrology and Earth System Sciences*, *27*(2), 559–576. <https://doi.org/10.5194/hess-27-559-2023>
- Jin, H., Vicente-Serrano, S. M., Tian, F., Cai, Z., Conradt, T., Boincean, B., et al. (2023). Higher vegetation sensitivity to meteorological drought in autumn than spring across European biomes. [Article]. *Communications Earth & Environment*, *4*(1), 299. <https://doi.org/10.1038/s43247-023-00960-w>
- Li, B., Beaudoin, H., & Rodell, M., & NASA/GSFC/HSL. (2020). GLDAS catchment land surface model L4 daily 0.25 × 0.25 degree GRACE-DA1 (version 2.2) [Dataset]. *Goddard Earth Sciences Data and Information Services Center (GES DISC)*. <https://doi.org/10.5067/TXBMLX370XX8>
- Li, D., An, L., Zhong, S., Shen, L., & Wu, S. (2024). Declining coupling between vegetation and drought over the past three decades. [Article]. *Global Change Biology*, *30*(1), e17141. <https://doi.org/10.1111/gcb.17141>
- Li, J., Wang, Z., Wu, X., Chen, J., Guo, S., & Zhang, Z. (2020b). A new framework for tracking flash drought events in space and time. [Article]. *Catena*, *194*, 104763. <https://doi.org/10.1016/j.catena.2020.104763>
- Li, M., Cao, S., Zhu, Z., Wang, Z., Myneni, R. B., & Piao, S. (2023a). Spatiotemporally consistent global dataset of the GIMMS normalized difference vegetation index (PKU GIMMS NDVI) from 1982 to 2022. [Article]. *Earth System Science Data*, *15*(9), 4181–4203. <https://doi.org/10.5194/essd-15-4181-2023>
- Li, M., Cao, S., Zhu, Z., Wang, Z., Myneni, R. B., & Piao, S. (2023b). Spatiotemporally consistent global dataset of the GIMMS normalized difference vegetation index (PKU GIMMS NDVI) from 1982 to 2022 (version 1.2) [Dataset]. *Spatiotemporally consistent global dataset of the GIMMS Normalized Difference Vegetation Index (PKU GIMMS NDVI) from 1982 to 2022 (Version 1.2)*. <https://doi.org/10.5281/zenodo.8253971>
- Li, M., Yang, Q. B., Zong, S. W., Wang, G. W., & Zhang, D. W. (2024). Understanding the spatiotemporal dynamics of vegetation drought and its time-lag link with teleconnection factors on the Loess Plateau. *Journal of Hydrology-Regional Studies*, *53*, 101778. <https://doi.org/10.1016/j.ejrh.2024.101778>
- Li, W., Migliavacca, M., Forkel, M., Denissen, J. M. C., Reichstein, M., Yang, H., et al. (2022). Widespread increasing vegetation sensitivity to soil moisture. [Article]. *Nature Communications*, *13*(1), 3959. <https://doi.org/10.1038/s41467-022-31667-9>
- Li, X., & Xiao, J. (2019). A global, 0.05-degree product of solar-induced chlorophyll fluorescence derived from OCO-2, MODIS, and reanalysis data. [Article]. *Remote Sensing*, *11*(5), 517. <https://doi.org/10.3390/rs11050517>
- Li, Y., Zhang, W., Schwalm, C. R., Gentile, P., Smith, W. K., Ciais, P., et al. (2023c). Widespread spring phenology effects on drought recovery of Northern Hemisphere ecosystems. [Article]. *Nature Climate Change*, *13*(2), 182–188. <https://doi.org/10.1038/s41558-022-01584-2>
- Liang, M. L., Yuan, X., Zhou, S. Y., & Ma, Z. S. (2023). Spatiotemporal evolution and nowcasting of the 2022 Yangtze River mega-flash drought. *Water*, *15*(15), 2744. <https://doi.org/10.3390/w15152744>
- Lloyd-Hughes, B. (2012). A spatio-temporal structure-based approach to drought characterisation. [Article]. *International Journal of Climatology*, *32*(3), 406–418. <https://doi.org/10.1002/joc.2280>
- Lu, M., Sun, H., Yang, Y., Xue, J., Ling, H., Zhang, H., & Zhang, W. (2024). Impact of hydro-meteorological conditions and flash drought duration on post-flash drought recovery time patterns. *Hydrology and Earth System Sciences Discussions*. <https://doi.org/10.5194/hess-2024-128>
- Lu, M. G., Sun, H. W., Cheng, L., Li, S. Y., Qin, H., Yi, S. Z., et al. (2024). Heterogeneity in vegetation recovery rates post-flash droughts across different ecosystems. *Environmental Research Letters*, *19*(7), 074028. <https://doi.org/10.1088/1748-9326/ad5570>
- Ma, F., & Yuan, X. (2024). Vegetation greening and climate warming increased the propagation risk from meteorological drought to soil drought at subseasonal timescales. *Geophysical Research Letters*, *51*(4), e2023GL107937. <https://doi.org/10.1029/2023gl107937>
- Martens, B., Miralles, D. G., Lievens, H., van der Schalie, R., de Jeu, R. A. M., Fernandez-Prieto, D., et al. (2017). GLEAM v3: Satellite-based land evaporation and root-zone soil moisture. *Geoscientific Model Development*, *10*(5), 1903–1925. <https://doi.org/10.5194/gmd-10-1903-2017>
- Mueller, L. M., & Bahn, M. (2022). Drought legacies and ecosystem responses to subsequent drought. [Review]. *Global Change Biology*, *28*(17), 5086–5103. <https://doi.org/10.1111/gcb.16270>
- Otkin, J. A., Svoboda, M., Hunt, E. D., Ford, T. W., Andersonson, M. C., Hain, C., & Basara, J. B. (2018). FLASH droughts A review and assessment of the challenges imposed by rapid-onset droughts in the United States. [Review]. *Bulletin of the American Meteorological Society*, *99*(5), 911–919. <https://doi.org/10.1175/bams-d-17-0149.1>
- Pendergrass, A. G., Meehl, G. A., Pulwarty, R., Hobbins, M., Hoell, A., AghaKouchak, A., et al. (2020). Flash droughts present a new challenge for subseasonal-to-seasonal prediction. [Article]. *Nature Climate Change*, *10*(3), 191–199. <https://doi.org/10.1038/s41558-020-0709-0>
- Pu, J., Roy, S., Knyazikhin, Y., & Myneni, R. (2023). Sensor-Independent LAI/FPAR CDR [Dataset]. *Sensor-Independent LAI/FPAR CDR*. <https://doi.org/10.5281/zenodo.8076539>
- Pu, J., Yan, K., Roy, S., Zhu, Z., Rautiainen, M., Knyazikhin, Y., & Myneni, R. B. (2024). Sensor-independent LAI/FPAR CDR: Reconstructing a global sensor-independent climate data record of MODIS and VIIRS LAI/FPAR from 2000 to 2022. [Article]. *Earth System Science Data*, *16*(1), 15–34. <https://doi.org/10.5194/essd-16-15-2024>

- Sabater, M. J. (2019). ERA5-Land hourly data from 1950 to present [Dataset]. *Copernicus Climate Change Service (C3S) Climate Data Store (CDS)*. <https://doi.org/10.24381/cds.e2161bac>
- Sato, H., Mizoi, J., Shinozaki, K., & Yamaguchi-Shinozaki, K. (2024). Complex plant responses to drought and heat stress under climate change. [Review]. *The Plant Journal*, *117*(6), 1873–1892. <https://doi.org/10.1111/tpj.16612>
- Schwalm, C. R., Anderegg, W. R. L., Michalak, A. M., Fisher, J. B., Biondi, F., Koch, G., et al. (2017). Global patterns of drought recovery. [Article]. *Nature*, *548*(7666), 202–205. <https://doi.org/10.1038/nature23021>
- Su, B. D., Huang, J. L., Fischer, T., Wang, Y. J., Kundzewicz, Z. W., Zhai, J. Q., et al. (2018). Drought losses in China might double between the 1.5°C and 2.0°C warming. *Proceedings of the National Academy of Sciences of the United States of America*, *115*(42), 10600–10605. <https://doi.org/10.1073/pnas.1802129115>
- Sungmin, O., & Orth, R. (2021). Global soil moisture data derived through machine learning trained with in-situ measurements [Article; Data Paper]. *Scientific Data*, *8*(1), 170. <https://doi.org/10.1038/s41597-021-00964-1>
- Sungmin, O., & Park, S. K. (2024). Global ecosystem responses to flash droughts are modulated by background climate and vegetation conditions. [Article]. *Communications Earth & Environment*, *5*(1), 88. <https://doi.org/10.1038/s43247-024-01247-4>
- Tang, J. W., Niu, B., Hu, Z. G., & Zhang, X. Z. (2024). Increasing susceptibility and shortening response time of vegetation productivity to drought from 2001 to 2021. *Agricultural and Forest Meteorology*, *352*, 110025. <https://doi.org/10.1016/j.agrformet.2024.110025>
- Tariq, A., Graciano, C., Sardans, J., Zeng, F., Hughes, A. C., Ahmed, Z., et al. (2024). Plant root mechanisms and their effects on carbon and nutrient accumulation in desert ecosystems under changes in land use and climate. [Review]. *New Phytologist*, *242*(3), 916–934. <https://doi.org/10.1111/nph.19676>
- Van Loon, A. F., Gleeson, T., Clark, J., Van Dijk, A., Stahl, K., Hannaford, J., et al. (2016). Drought in the anthropocene. *Nature Geoscience*, *9*(2), 89–91. <https://doi.org/10.1038/ngeo2646>
- Wang, A., Lettenmaier, D. P., & Sheffield, J. (2011). Soil moisture drought in China, 1950–2006. *Journal of Climate*, *24*(13), 3257–3271. <https://doi.org/10.1175/2011jcli3733.1>
- Wang, Y., & Yuan, X. (2021). Anthropogenic speeding up of south China flash droughts as exemplified by the 2019 summer-autumn transition season. [Article]. *Geophysical Research Letters*, *48*(9), e2020GL091901. <https://doi.org/10.1029/2020gl091901>
- Wang, Y. M., & Yuan, X. (2023). High temperature accelerates onset speed of the 2022 unprecedented flash drought over the Yangtze River Basin. [Article]. *Geophysical Research Letters*, *50*(22), e2023GL105375. <https://doi.org/10.1029/2023GL105375>
- Xi, X., Liang, M., & Yuan, X. (2024). Increased atmospheric water stress on gross primary productivity during flash droughts over China from 1961 to 2022. [Article]. *Weather and Climate Extremes*, *44*, 100667. <https://doi.org/10.1016/j.wace.2024.100667>
- Xu, H. J., Wang, X. P., Zhao, C. Y., & Yang, X. M. (2018). Diverse responses of vegetation growth to meteorological drought across climate zones and land biomes in northern China from 1981 to 2014. *Agricultural and Forest Meteorology*, *262*, 1–13. <https://doi.org/10.1016/j.agrformet.2018.06.027>
- Xu, H. T., Chen, H. W., Chen, D. L., Wang, Y. P., Yue, X., He, B., et al. (2024). Global patterns and drivers of post-fire vegetation productivity recovery. *Nature Geoscience*, *17*(9), 874–881. <https://doi.org/10.1038/s41561-024-01520-3>
- Xu, K., Yang, D., Yang, H., Li, Z., Qin, Y., & Shen, Y. (2015). Spatio-temporal variation of drought in China during 1961–2012: A climatic perspective. [Article]. *Journal of Hydrology*, *526*, 253–264. <https://doi.org/10.1016/j.jhydrol.2014.09.047>
- Yan, K., Wang, J., Weiss, M., & Myneni, R. B. (2023). A high-quality reprocessed MODIS leaf area index dataset (HiQ-LAI) (version 1) [Dataset]. *A High-Quality Reprocessed MODIS Leaf Area Index Dataset (HiQ-LAI) (Version 1)*. <https://doi.org/10.5281/zenodo.8296768>
- Yao, T., Liu, S., Hu, S., & Mo, X. (2022). Response of vegetation ecosystems to flash drought with solar-induced chlorophyll fluorescence over the Hai River Basin, China during 2001–2019. [Article]. *Journal of Environmental Management*, *313*, 114947. <https://doi.org/10.1016/j.jenvman.2022.114947>
- Yao, Y., Fu, B. J., Liu, Y. X., Li, Y., Wang, S., Zhan, T. Y., et al. (2022). Evaluation of ecosystem resilience to drought based on drought intensity and recovery time. *Agricultural and Forest Meteorology*, *314*, 108809. <https://doi.org/10.1016/j.agrformet.2022.108809>
- Yao, Y., Liu, Y. X., Zhou, S., Song, J. X., & Fu, B. J. (2023). Soil moisture determines the recovery time of ecosystems from drought. *Global Change Biology*, *29*(13), 3562–3574. <https://doi.org/10.1111/gcb.16620>
- Yin, J. B., Gentine, P., Slater, L., Gu, L., Pokhrel, Y., Hanasaki, N., et al. (2023). Future socio-ecosystem productivity threatened by compound drought-heatwave events. *Nature Sustainability*, *6*(3), 259–272. <https://doi.org/10.1038/s41893-022-01024-1>
- Yuan, X., Wang, L. Y., Wu, P. L., Ji, P., Sheffield, J., & Zhang, M. (2019). Anthropogenic shift towards higher risk of flash drought over China. *Nature Communications*, *10*(1), 4661. <https://doi.org/10.1038/s41467-019-12692-7>
- Yuan, X., Wang, Y., Ji, P., Wu, P., Sheffield, J., & Otkin, J. A. (2023). A global transition to flash droughts under climate change. [Article]. *Science*, *380*(6641), 187–191. <https://doi.org/10.1126/science.abn6301>
- Zeng, Z., Wu, W., Penuelas, J., Li, Y., Jiao, W., Li, Z., et al. (2023). Increased risk of flash droughts with raised concurrent hot and dry extremes under global warming. [Article]. *Npj Climate and Atmospheric Science*, *6*(1), 134. <https://doi.org/10.1038/s41612-023-00468-2>
- Zhang, M., & Yuan, X. (2020). Rapid reduction in ecosystem productivity caused by flash droughts based on decade-long FLUXNET observations. *Hydrology and Earth System Sciences*, *24*(11), 5579–5593. <https://doi.org/10.5194/hess-24-5579-2020>
- Zhang, Y., Cai, M., Xiao, X., Yang, X., Migliavacca, M., Basara, J., et al. (2024). Immediate and lagged vegetation responses to dry spells revealed by continuous solar-induced chlorophyll fluorescence observations in a tall-grass prairie. [Article]. *Remote Sensing of Environment*, *305*, 114080. <https://doi.org/10.1016/j.rse.2024.114080>
- Zhao, Y., Xiong, L., Yin, J., Zha, X., Li, W., & Han, Y. (2024). Understanding the effects of flash drought on vegetation photosynthesis and potential drivers over China. [Article]. *Science of the Total Environment*, *931*, 172926. <https://doi.org/10.1016/j.scitotenv.2024.172926>
- Zheng, L., Lu, J. Z., & Chen, X. L. (2024). Drought offsets the vegetation greenness-induced gross primary productivity from 1982 to 2018 in China. *Journal of Hydrology*, *632*, 130881. <https://doi.org/10.1016/j.jhydrol.2024.130881>